phys. stat. sol. (b) **245**, No. 10, 2164–2168 (2008) / **DOI** 10.1002/pssb.200879583

physica status solidi b
www.pss-b.com
basic solid state physics

Theory of ultrafast intraband relaxation in carbon nanotubes

Matthias Hirtschulz[1,*], Frank Milde[1], Ermin Malic[1], Christian Thomsen[2], Stephanie Reich[3], and Andreas Knorr[1]

[1] Institut für Theoretische Physik, Technische Universität Berlin, 10623 Berlin, Germany
[2] Institut für Festkörperphysik, Technische Universität Berlin, 10623 Berlin, Germany
[3] Fachbereich Physik, Freie Universität Berlin, 14195 Berlin, Germany

Received 29 April 2008, revised 13 June 2008, accepted 20 June 2008
Published online 26 August 2008

PACS 73.22.–f, 78.47.–p, 78.67.Ch

* Corresponding author: e-mail matthias@itp.physik.tu-berlin.de, Phone: +49-30-31423762, Fax: +49-30-31421130

Ultrafast intraband carrier relaxation in carbon nanotubes can be described by Carbon Nanotube Bloch Equations (CNBE) treating the Coulomb interaction beyond the Hartree-Fock level to include carrier-carrier scattering. We obtain equations of motion for carrier densities and two-particle carrier correlations that are solved numerically. The complex non-Markovian relaxation dynamics of hot electrons is calculated for various carbon nanotubes of different diameter and chirality. All calculated nanotubes show an ultrafast relaxation to equilibrium within approximately 100 femtoseconds. The observed relaxation is only weakly dependent on chirality, but depends on the diameter of the nanotube. With increasing diameter of the CNT the relaxation is slowed down, because of the weaker Coulomb interaction in larger diameter CNT. Additionally, we find oscillations of the electron plasma that are due to memory effects in the electron equilibration.

1 Introduction Single wall carbon nanotubes are quasi-onedimensional systems that have unique optical and electronic properties. They are promising candidates for applications in nanoscale electronic devices [1,2]. A sound and fundamental understanding of ultrafast and nonlinear properties of these nanoscale systems is necessary to build future (opto-)electronic devices. In recent years several time-domain spectroscopic studies have been carried out [3–5], but a complete (theoretical) understanding is lacking and there are still several controversial results in ultrafast spectroscopy (see [6] and references therein). In this contribution, as a first step towards a microscopic theory of ultrafast processes in carbon nanotubes (CNTs), we present an analysis of the electronic intraband relaxation dynamics in CNTs. We obtain the Coulomb scattering induced intraband relaxation of excited carriers within the framework of density matrix theory [7,8]. The Carbon Nanotube Bloch Equations (CNBEs) approach [9–11] is extended beyond the Hartree-Fock level to include Coulomb correlation effects that lead to carrier relaxation and plasma screening. In Ref. [9] we have already addressed linear and non-linear properties of CNTs on the Hartree-Fock level suitable for off-resonant and not too strong optical excitation. Here, we extend the calculation by treating a non-Markovian second order Born description of Coulomb correlations. Within a one-band model we find that an initial non-equilibrium carrier distribution relaxes to a quasi-equilibrium on a 100 fs timescale, i.e. carrier-carrier intraband thermalization is relatively fast (depending on density) and electron-phonon scattering acts on longer timescales [4]. We performed calculations for the CNTs of the $2n_1 + n_2 = 29$ branch and find only a minor chirality dependence in the carrier dynamics (Section 3). However, we predict a more pronounced dependence on the diameter of the CNT.

2 Theoretical background Interaction mechanisms such as electron-electron or electron-phonon scattering are responsible for ultrafast intra- and inter-subband relaxation of excited electronic states, typically on a pico- to femtosecond timescale. These processes cannot be described within a mean-field theory [9]. Density matrix theory is an ideal candidate to describe ultrafast non-linear dynamics [12] in semiconductor materials as it can be easily extended beyond the Hartree-Fock level. Starting

point of the theory is the Heisenberg equation of motion (EOM) $\langle \dot{O} \rangle = \frac{i}{\hbar} \langle [H, O] \rangle$, where the expectation value of an observable O is computed with the density matrix ρ: $\langle O \rangle = \mathrm{Tr}\{O\rho\}$. When computing the dynamics of microscopic quantities (expressed in terms of creation and annihilation operators $a^\dagger_{\lambda \mathbf{k}}$ and $a_{\lambda \mathbf{k}}$) such as occupation probabilities $n^\lambda_{\mathbf{k}} = \langle a^\dagger_{\lambda \mathbf{k}} a_{\lambda \mathbf{k}} \rangle$ in band $\lambda = c, v$ or transition probability amplitudes $p_{\mathbf{k}} = \langle a^\dagger_{v\mathbf{k}} a_{c\mathbf{k}} \rangle$ the commutator with the Hamiltonian must be evaluated. The computation leads to an infinite hierarchy of higher order quantities that can be truncated in a systematic way [7]. In Sections 2.1 and 2.2 we introduce the system Hamiltonian and the resulting EOMs for $n_{\mathbf{k}}$ and density correlations C^{12}_{34}.

2.1 Hamilton operator The full Hamilton operator of the CNT system $H = H_f + H_{ee}$ consists of a free contribution H_f and a Coulomb interaction term H_{ee}. The free part H_f includes the single-particle Hamiltonian with the tight binding band structure $E(1) := E_{\lambda_1}(\mathbf{k}_1)$ (with tight-binding parameters: $\gamma_0 = -2.84$ eV, $a_0 = 0.2461$ nm, only on-site interaction [13]) and the electron light interaction (in second quantization):

$$H_f = \sum_1 E(1) a^\dagger_1 a_1 - \frac{e_0 \hbar}{i m_0} \mathbf{A}_t \cdot \sum_{1,2} \mathbf{M}_{12} a^\dagger_1 a_2. \qquad (1)$$

Here, we use the compound quantum number $1 = (\lambda_1, \mathbf{k}_1)$, where $\mathbf{k}_1$ is the two-dimensional electron momentum in zone-folding approximation. $\mathbf{M}_{12}$ are the optical matrix elements [14]. m_0 is the free electron mass and e_0 the elementary charge. The Coulomb Hamilton operator H_{ee} has the form:

$$H_{ee} = \frac{1}{2} \sum_{1,2,3,4} V^{12}_{34} a^\dagger_1 a^\dagger_2 a_4 a_3 \qquad (2)$$

with Coulomb matrix elements $V^{12}_{34} = \langle 1|\langle 2|V(\mathbf{r} - \mathbf{r}')|3\rangle|4\rangle$, the regularized Coulomb potential $V(\mathbf{r} - \mathbf{r}')$ and the single-particle tight binding wave functions $\langle \mathbf{r}|1\rangle$ [9].

2.2 Carrier densities and electron correlations In the Heisenberg EOM, the elements of the one-particle density matrix $f_{12} := \langle a^\dagger_1 a_2 \rangle$ couple to two-particle density matrices $S^{12}_{34} := \langle a^\dagger_1 a^\dagger_2 a_3 a_4 \rangle$. When going beyond the Hartree-Fock level the two-particle quantities S^{12}_{34} are not factorized into one-particle quantities, but calculated dynamically. The two-particle quantities couple to three-particle quantities, that are factorized into two- and one--particle contributions [15]. In order to analyze the influence of the higher order contributions in comparison to the Hartree-Fock results, the Coulomb correlations are introduced as the deviations of the two-particle density matrix from the Hartree-Fock factorized parts: $C^{12}_{34} := S^{12}_{34} - f_{14} f_{23} + f_{13} f_{24}$. These quantities are the source terms for the population dynamics:

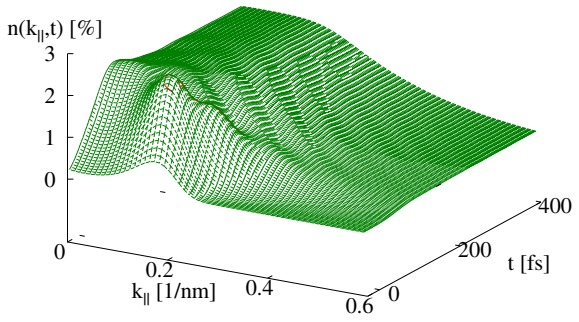

Figure 1 Carrier dynamics $n(k_{\shortparallel}, t)$ of the (11,6) CNT for $\sigma_t = 28$ fs and $\sigma_E = 12$ meV. The generation rate is energetically centered at $E_0 = 0.715$ meV corresponding to $k_{\shortparallel} \approx 0.18$ 1/nm.

$$\dot{n}_{\mathbf{k}}|^{corr} = \frac{2}{\hbar} \mathrm{Im} \left\{ \sum_{\mathbf{k}',\mathbf{q}} V_{(\mathbf{k}+\mathbf{q},\mathbf{k}')} C_{(\mathbf{k}+\mathbf{q},\mathbf{k}')} \right\}. \qquad (3)$$

The correlations dynamics are given by (for a one-band model we can drop the single band quantum number $\lambda = c$ for the conduction band):

$$\dot{C}_{(\mathbf{k}+\mathbf{q},\mathbf{k}')} = i\omega_{(\mathbf{k}+\mathbf{q},\mathbf{k}')} C_{(\mathbf{k}+\mathbf{q},\mathbf{k}')} + A_1. \qquad (4)$$

For reasons of clarity we introduced the abbreviation: $X_{(\mathbf{k}+\mathbf{q},\mathbf{k}')} := X^{\mathbf{k}+\mathbf{q},\mathbf{k}'}_{\mathbf{k},\mathbf{k}'+\mathbf{q}}$ and $\omega_{(\mathbf{k}+\mathbf{q},\mathbf{k}')} := (E_c(\mathbf{k}+\mathbf{q}) + E_c(\mathbf{k}') - E_c(\mathbf{k}) - E_c(\mathbf{k}'+\mathbf{q}))/\hbar$. A_1 is the Boltzmann like scattering contribution that is the driving force of the Coulomb correlation:

$$A_1 = W_{(\mathbf{k}'+\mathbf{q},\mathbf{k})} [n_{\mathbf{k}+\mathbf{q}} n_{\mathbf{k}'} (1 - n_{\mathbf{k}})(1 - n_{\mathbf{k}'+\mathbf{q}}) - n_{\mathbf{k}'+\mathbf{q}} n_{\mathbf{k}} (1 - n_{\mathbf{k}'})(1 - n_{\mathbf{k}+\mathbf{q}})] \qquad (5)$$

with $W_{(\mathbf{k}'+\mathbf{q},\mathbf{k})} = V_{(\mathbf{k}'+\mathbf{q},\mathbf{k})} - V^{\mathbf{k},\mathbf{k}'+\mathbf{q}}_{\mathbf{k}',\mathbf{k}+\mathbf{q}}$. The first and the second term describe in and out scattering events from electron states with momentum $\mathbf{k} + \mathbf{q}$ and $\mathbf{k}'$ to states with momentum $\mathbf{k}$ and $\mathbf{k}' + \mathbf{q}$, respectively. The memory effects contained in these coupled equations (Eqs. (3) and (4)) can be understood when formally integrating Eq. (4). In combination with Eq. ((3)) one obtains an integro-differential equation for the populations clearly showing the non-Markovian character of the theory. Note, that the description of screening effects [16] or polarization relaxation [15] are beyond the scope of this paper but will be addressed in future work. Screening of the Coulomb interaction by an external dielectric constant would lead to less effective scattering and slower themalization of the

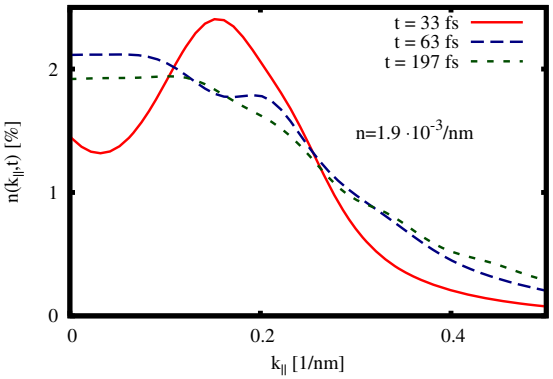

Figure 2 Carrier population of the (11,6) CNT at three different times for the same excitation conditions as in Fig. 1 (with total electron density of $n = 1.9 \cdot 10^{-3} 1/\text{nm}$). After 200 fs the carrier distribution has almost reached its equilibrium (short-dashed line) with electronic temperature T ≈ 560 K and chemical potential of $\mu \approx 0.2$ eV.

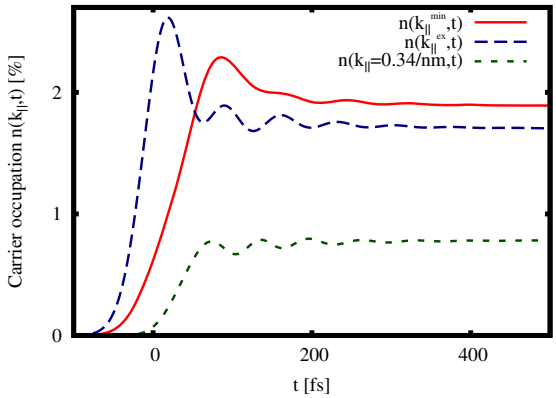

Figure 3 Carrier occupation $n(k_{\shortparallel} = \text{const.}, t)$ of the (11,6) CNT over time for three different values of the wave vector $k_{\shortparallel}$. An exponential fit yields a relaxation time $\tau_{\text{ex}} \approx 26$ fs (long-dashed line) and $\tau_{\text{min}} \approx 60$ fs (solid line). The short-dashed line is non-exponential.

initial non-equilibrium electron distribution. The polarization dephasing times are expected to be in the same order of magnitude as the present relaxation dynamics. The impact of electron-phonon scattering on the ultrafast dynamics can be neglected here, since the intrasubband thermalization due to carrier-carrier scattering takes place on a shorter time scale at sufficiently low temperatures [4, 17]. In order to model the generation of carriers by an optical field, a semiclassical generation rate is included into Eq. (4). This ensures a continuous build-up of the correlation, as opposed to a fixed initial carrier distribution [18]. The generation rate is assumed to be Gaussian in time and reciprocal space:

$$\dot{n}_{\mathbf{k}}|^{gen} = g_0 e^{-\frac{t^2}{2\sigma_t^2}} e^{-\frac{(E_{\mathbf{k}}-E_0)^2}{2\sigma_E^2}}. \qquad (6)$$

This ansatz for a non-equilibrium pumping mechanism is necessary as only the unexcited CNT has vanishing carrier densities ($n_{\mathbf{k}}|^{corr} = 0$) and correlations ($C_{(\mathbf{k}+\mathbf{q},\mathbf{k}')} = 0$).

3 Results The above EOM for the correlations $C_{(\mathbf{k}+\mathbf{q},\mathbf{k}')}$ and carrier densities $n_{\mathbf{k}}$ are solved numerically for various CNTs. The numerical convergence of the shown results was tested with respect to the discretization in time (typically 0.1 fs) and reciprocal space (typically 10^{-3}/nm) as well as with respect to the size of the considered subband. Figure 1 shows the carrier density dynamics $n_{\mathbf{k}}(t)$ of a (11,6) CNT within the first 400 fs after a carrier generation with $\sigma_t = 28$ fs and $\sigma_E = 12$ meV (cp. Eq. (6)). The initial non-equilibrium carrier distribution peaked at $k_{\shortparallel} \neq 0$ rapidly evolves into an equilibrium Fermi-like funtion centered around $k_{\shortparallel} \approx 0$. Furthermore, we observe temporal and wave number related oscillations in the electron plasma distribution. Such oscillations are connected to the wave like properties of the electron plasma beyond a Markovian approximation. Figure 2 shows the carrier population $n_{\mathbf{k}}$ at different times after the carrier generation in more detail. Note that, the minimum of the band $\omega_c(\mathbf{k})$ is located at $k_{\shortparallel} \approx 0$. Initially, the carrier distribution at the band minimum is low compared to the maximum occupation at higher energies in the band. As time evolves, due to carrier-carrier scattering the initial sharp electron distribution (t = 0 fs) is broadened and the carriers are transferred to the band minimum. After 100-200 fs the thermalization of the non-equilibrium carrier distribution is completed. This is in good agreement with experimental findings [4] predicting an intraband relaxation time of 130 fs. A least-square fit of the final equilibrium carrier distribution gives an electronic temperature of T ≈ 560 K and chemical potential of $\mu \approx 0.2$ eV. As we see from Fig. 1, the non-linear carrier relaxation dynamics of an excited CNT can not be described by a single relaxation time τ. To give at least a simplified description of the dynamics we introduce two relaxation times τ_{ex} and τ_{min}. τ_{ex} is the exponential relaxation time at wavevector $k_{\shortparallel} = k_{\shortparallel}^{\text{ex}}$ where the excitation is centered (20 meV above the band minimum troughout this work). τ_{min} is the exponential relaxation time at wavevector $k_{\shortparallel} = k_{\shortparallel}^{\text{min}}$ where the band minimum is located. The relaxation times are obtained by a least-square fit of an exponential fitting function. In Fig. 3 the relaxation dynamics at $k_{\shortparallel} = k_{\shortparallel}^{\text{min}}$ (solid line) and at $k_{\shortparallel} = k_{\shortparallel}^{\text{ex}}$ (long-dashed line) are compared: $\tau_{\text{ex}} \approx 26$ fs and $\tau_{\text{min}} \approx 60$ fs are found. Note also, that the relaxation dynamics for some $n_{\mathbf{k}}(t)$ are strongly non-exponential (short-dashed line in Fig. 3). This complex behavior does not only result from the non-Markovian EOM, but also occurs because the relaxation dynamics depend on the carrier density generated in the band. In Fig. 4 we compare the relaxation dynamics of the (11,6) CNT at $k_{\shortparallel} = k_{\shortparallel}^{\text{ex}}$ for different amplitudes g_0 of the generation rate $\dot{n}_{\mathbf{k}}|^{gen}$ (Eq.

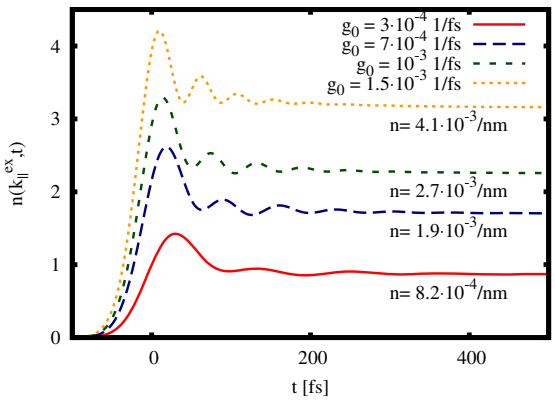

Figure 4 Carrier dynamics of the (11,6) CNT at $k_{\shortparallel} = k_{\shortparallel}^{\mathrm{ex}}$ for different generation rate amplitudes g_0. With increasing amplitude from $g_0 = 3 \cdot 10^{-4} 1/$ fs to $g_0 = 1.5 \cdot 10^{-3} 1/$ fs the decay time decreases from $\tau_{\mathrm{ex}} = 38$ fs to $\tau_{\mathrm{ex}} = 24$ fs, while the period of the oscillations T_{ex} decreases from $T_{\mathrm{ex}} = 120$ fs to $T_{\mathrm{ex}} = 50$ fs.

(6)). When the generation rate amplitude is varied from $g_0 = 0.3/\mathrm{ps}$ to $g_0 = 1.5/\mathrm{ps}$ (Fig. 4) the generation is enhanced and consequently the relaxation times decrease (more scattering partners are present) from $\tau_{\mathrm{ex}} = 38$ fs to $\tau_{\mathrm{ex}} = 24$ fs. Furthermore, the periods of the carrier oscillations T_{ex} decrease as g_0 is increased. At $g_0 = 0.3/\mathrm{ps}$ we find a period of $T_{\mathrm{ex}} = 120$ fs that is more than twice as long as $T_{\mathrm{ex}} = 50$ fs for $g_0 = 1.5/\mathrm{ps}$.

We have done similar calculations for all CNTs of the $2n_1 + n_2 = 29$ branch (Table 1). The qualitative behavior of the relaxation dynamics is very similar to that of the (11,6) CNT (cp. Fig. 1). Within the branch the relaxation times ($\tau_{\mathrm{ex}} \sim 23$ fs,$\tau_{\mathrm{min}} \sim 45$ fs) and the oscillation periods $T_{\mathrm{ex}} \sim 80$ fs are nearly independent of chirality. While relaxation dynamics seem not to strongly depend

Table 1 Relaxation times τ_{ex} and τ_{min} and periods of plasma oscillations T_{ex} for CNTs (diameter d, chiral angle θ) of the $2n_1 + n_2 = 29$ branch and the (11,6), (22,12) and (44,24) CNTs of same chirality.

n_1	n_2	d [nm]	$\theta[^\circ]$	τ_{ex} [fs]	τ_{min} [fs]	T_{ex} [fs]
10	9	1.29	28.3	23	45	76
11	7	1.23	22.7	24	45	75
12	5	1.19	16.6	23	45	80
13	3	1.15	10.2	23	45	80
14	1	1.14	3.4	23	45	80
11	6	1.17	20.4	23	49	81
22	12	2.34	20.4	36	56	97
44	24	4.68	20.4	51	37	137

on chirality we find a dependence of the relaxation times and oscillation period on the diameter of the CNT. We have done calculations for the (11,6), (22,12) and (44,24), which all have the same chirality of $\theta = 20.4^\circ$ but diameters ranging from ~ 1.2 nm to ~ 4.7 nm (Table 1). For the same excitation conditions as above we find that the relaxation time τ_{ex} increases with diameter (Table 1). This is due to the weaker Coulomb interaction in larger diameter CNTs (matrix element $V_{(\mathbf{k}+\mathbf{q},\mathbf{k}')}$ decreases with increasing diameter).

4 Conclusions In summary, we have calculated the ultrafast intraband relaxation dynamics of excited carriers in CNTs. We employed the Carbon Nanotube Bloch Equation (CNBE) approach [9], including non-Markovian second-order Born correlation effects that lead to carrier-carrier scattering. Typically, we find an ultrafast thermalization of carriers on a timescale of 100 fs for various CNTs of different chirality and diameter. This result agrees well with recent experiments of Lauret et al. [4]. From our studies we find nearly no chirality but a considerable diameter dependence for the calculated CNTs. Non-Markovian features are manifested in oscillations of the electron plasma occupation. We find oscillations with periods in the range of 70-140 fs. A next step, to analyze optical properties, is to consider the formation of excitons [9] and their Coulomb quantum kinetics within the CNBEs. Further studies could also investigate the influence of the length of the generating pulse on the relaxation dynamics to deconvolve relaxation and pulse contributions to the dynamics.

Acknowledgements Support from the Cluster of Excellence 'Unifying Concepts in Catalysis' (DFG) is acknowledged. We thank Studienstiftung des Deutschen Volkes and DFG for financial support.

References

[1] N. Mason, M. Biercuk, and C. Marcus, Science **303**(5658), 655 (2004).
[2] J. Misewich, R. Martel, P. Avouris, J. Tsang, S. Heinze, and J. Tersoff, Science **300**(5620), 783 (2003).
[3] T. Hertel and G. Moos, Phys. Rev. Lett. **84**(21), 5002 (2000).
[4] J. S. Lauret, C. Voisin, G. Cassabois, C. Delalande, P. Roussignol, O. Jost, and L. Capes, Phys. Rev. Lett. **90**(5), 057404 (2003).
[5] Y. Ma, L. Valkunas, S. Dexheimer, S. Bachilo, and G. Fleming, Phys. Rev. Lett. **94**(15), 157402 (2005).
[6] B. F. Habenicht, C. F. Craig, and O. V. Prezhdo, Phys. Rev. Lett. **96**(18), 187401 (2006).
[7] V. Axt and A. Stahl, Z. Phys. B **93**(2), 195 (1994).
[8] H. Haug and S. Koch, Quantum Theory of the Optical and Electronic Properties of Semiconductors (World Scientific Publishing Co., 2004).
[9] M. Hirtschulz, F. Milde, E. Malić, S. Butscher, C. Thomsen, S. Reich, and A. Knorr, Phys. Rev. B **77**(3), 035403 (2008).
[10] E. Malić, M. Hirtschulz, F. Milde, Y. Wu, J. Maultzsch, T. F. Heinz, A. Knorr, and S. Reich, Phys. Rev. B **77**(4), 045432 (2008).
[11] E. Malic, M. Hirtschulz, F. Milde, Y. Wu, J. Maultzsch, T. Heinz, A. Knorr, and S. Reich, phys. stat. sol. (b) **244**(11), 4240 (2007).
[12] S. Butscher, F. Milde, M. Hirtschulz, E. Malić, and A. Knorr, Appl. Phys. Lett. **91**, 203103 (2007).

[13] S. Reich, C. Thomsen, J. Maultzsch, and M. Janina, Carbon Nanotubes: Basic Concepts and Physical Properties (Wiley-VCH, 2004).
[14] E. Malić, M. Hirtschulz, F. Milde, A. Knorr, and S. Reich, Phys. Rev. B **74**(19), 195431 (2006).
[15] M. Lindberg and S. W. Koch, Phys. Rev. B **38**(5), 3342–3350 (1988).
[16] E. Heiner, phys. stat. sol. (b) **153**(1), 295 (1989).
[17] B. Habenicht, H. Kamisaka, K. Yamashita, and O. Prezhdo, Nano Lett. **7**(11), 3260 (2007).
[18] F. Prengel and E. Schöll, Phys. Rev. B **59**(8), 5806 (1999).

